

Molecule/Electrode Interface Energetics in Molecular Junction: a “Transition Voltage Spectroscopy” Study

Guillaume Ricœur, Stéphane Lenfant, David Guérin, Dominique Vuillaume**

Institut d'Electronique Microélectronique et Nanotechnologie (IEMN), CNRS,

University of Lille, B.P. 60069, Avenue Poincaré, F-59652, Villeneuve d'Ascq, France

ABSTRACT: We assess the performances of the transition voltage spectroscopy (TVS) method to determine the energies of the molecular orbitals involved in the electronic transport through molecular junctions. A large number of various molecular junctions made with alkyl chains but with different chemical structure of the electrode/molecule interfaces are studied. In the case of molecular junctions with “clean, unoxidized” electrode/molecule interfaces, i.e. alkylthiols and alkenes directly grafted on Au and hydrogenated Si, respectively, we measure transition voltages in the range 0.9 – 1.4 V. We conclude that the TVS method allows estimating the onset of the tail of the LUMO density of states, at energy located 1.0 – 1.2 eV above the electrode Fermi energy. For “oxidized” interfaces (e.g. the same monolayer measured with Hg or eGaIn drops, or monolayers formed on a slightly oxidized silicon substrate), lower transition voltages (0.1 - 0.6 V) are systematically measured. These values are explained by the presence of oxide-related density of states at energies lower than the HOMO/LUMO of the molecules. As such, the TVS

method is a useful technique to assess the quality of the molecule/electrode interfaces in molecular junctions.

KEYWORDS: SAM; Self Assembled Monolayer; TVS; Transition Voltage Spectroscopy; Molecular junction; Molecular electronic; Conducting AFM; Mercury probe; eGaIn; Alkene; Alkylthiol; Alkyltrichlorosilane; tunneling barrier.

1. INTRODUCTION

Over the past decade, numerous fabrication and measurement techniques have been developed to characterize the charge transport in metal/Self Assembled Monolayer (SAM)/metal junctions including scanning probes (STM, C-AFM), mechanically-controlled break junctions (e-beam lithographed and STM-based), nanopore-based junctions, metallic wire cross-bars, top electrode deposited by transfer printing, or using “liquid” contact (e.g. Hg drop) - (for a review see reference¹). This abundant literature on the subject shows an important dispersion of the measured conductance for the same type of molecules.² This dispersion is related to the fact that the conductance of the molecular junctions is strongly sensitive to the chemical nature and structural details of the molecule/electrode interfaces and to the molecular organization in the monolayer. These last few years, the “Transition Voltage Spectroscopy” technique (or TVS)^{3;4;5;6;7} has been used more frequently to estimate the energy barrier height at the electrode/molecule interface (i.e. the energy offset between the Fermi energy of the metal electrode and one of the molecular orbitals of the molecule). In this method, the energy barrier height is directly estimated from current-voltage (I-V) measurements, by plotting the I-V data in the form of a Fowler-Nordheim plot ($\ln(I/V^2)$ vs. $1/V$). In the classical interpretation of electron transport through a tunneling barrier,^{4;8} the voltage at which a minimum is observed in this plot

represents the transition voltage V_T between the direct and Fowler-Nordheim tunneling regime. Applied to molecular junctions, it is shown that V_T can give an estimation of the energy position of the molecular orbital (relative to the Fermi energy of the electrodes) involved in the transport mechanism, via a simple relation-ship $\Phi = \alpha V_T$, where α depends on several device parameters (symmetry of the junction in particular) ($0.8 < \alpha < 2$).^{9;10} Albeit, the fact that the exact value of α and the physical origin of V_T are still under debate,^{9;10;11;12} TVS has become an increasingly popular tool in molecular electronics.

Beebe et al.^{3;4} compare the V_T measured on SAM of alkylthiol molecules by two techniques: conducting-AFM (alkyl chains with 6 to 12 carbon atoms) and cross wires (12 to 18 carbon atoms). They observe a constant V_T with the length of the molecules: $V_T = 1.22 \pm 0.05$ V. Another work⁶ on alkyldithiol molecules characterized by electromigrated nanogap junction at 4.2 K reports also a constant $V_T = 1.9 \pm 0.1$ V with length of molecules for 8 to 12 carbon atoms. Using STM-based break junctions with alkyldithiols, *Guo et al.*¹³ report V_T in the range 1 - 1.5 eV. Recently, *Clement et al.*, also report V_T around 1.2 – 1.8 V for junctions made of a small amount (~ 80) of alkylthiols (12 carbon atoms) grafted on a tiny monocrystalline Au nanodot (< 8 nm in diameter) contacted by a C-AFM tip.¹⁴

Albeit the TVS approach is mainly applied on molecular junctions with thiolated molecules on gold substrate, one group^{15;16} reports very small V_T (about 0.2 V) for alkyl molecules on silicon substrates. Electron transport through silicon/molecule interface states is suggested to explain this low value.

Here, to assess the performances and potential of the TVS method, we extensively use this method on a large number of molecular junctions with different type of molecule/electrode interfaces, different test-beds and different lateral sizes (from few tens of nm to μ m). As top

contact of the molecular junctions, we use various techniques: conducting-AFM,¹⁷ aluminum evaporation through a shadow mask,¹⁸ “liquid” contact by eutectic GaIn¹⁹ or mercury²⁰ drop and micropore-based junctions (Figures 1a to 1e). We apply these contacting techniques to three families of SAM: alkylthiol ($\text{CH}_3-(\text{CH}_2)_{n-1}\text{SH}$ with $n=4$ to 18) on gold surfaces, alkyltrichlorosilane ($\text{CH}_3-(\text{CH}_2)_{n-1}\text{SiCl}_3$) with $n=8$ to 12 on silicon with native oxide and alkene ($\text{CH}_2=\text{CH}-(\text{CH}_2)_{n-3}-\text{CH}_3$ with $n=6$ to 10) grafted on hydrogenated silicon (Figure 1f). As a result, 10 different types of molecular junctions (with different chemical nature of the electrode/molecule interface, lateral size, and chain length) are characterized. The chosen molecules, based on alkyl chains, constitute an interesting case study for TVS, because (i) their HOMO (Highest Occupied Molecular Orbital) - LUMO (Lowest Unoccupied Molecular Orbital) gap remains constant with the number of methylene units in the chain (as soon as larger than 4)^{21;22}, (ii) the electronic transport in the junction is a non resonant tunneling²¹. In many previous works, only one bias polarity is used to determine V_T . In this study, we determine systematically V_{T+} at positive bias and V_{T-} at negative bias, since these values can be used to determine the energy position of the molecular orbital involved in the electrical transport¹¹ and the degree of symmetry/asymmetry of the junction.²³ We also discuss and compare the TVS results with independent measurements of the energetics of the molecular junctions (by UPS and IPES) when such data are available in literature for the same type of molecular junctions.

2. EXPERIMENTAL METHODS

We fabricated several molecular junctions belonging to three different groups. The first group referred to as “oxide free” junctions corresponds to SAMs of alkylthiol on gold and alkene on hydrogenated silicon substrates, contacted with a gold C-AFM tip: $\text{Au}_{\text{sub}}-\text{S}-\text{C}_n\text{H}_{2n+1}/\text{Au}_{\text{tip}}$ ($n=4,6,8,12,14,16,18$), and $\text{Si}-\text{C}_n\text{H}_{2n+1}/\text{Au}_{\text{tip}}$ ($n=6,8,10$), where “-” denotes an interface with a

chemical bond, and "/" a non-covalent, or mechanical interface. The second group referred to as "oxidized top contact" corresponds to the same SAMs contacted with eutectic GaIn (eGaIn), Hg drop or evaporated Al contacts. In this group, we measured 4 different types of junctions: $\text{Au}_{\text{sub}}\text{-S-C}_n\text{H}_{2n+1}\text{//Ga}_2\text{O}_3\text{/eGaIn}$, $\text{Si-C}_n\text{H}_{2n+1}\text{//Ga}_2\text{O}_3\text{/eGaIn}$, $\text{Si-C}_n\text{H}_{2n+1}\text{//HgO/Hg}$ and $\text{Si-C}_n\text{H}_{2n+1}\text{//Al}_2\text{O}_3\text{/Al}$, where "/" denotes an intimate contact at the interface, e.g. the interface between a metal and its oxide, or between a SAM and an evaporated metal. Both eGaIn and Hg drops have a very thin superficial oxide, likely Ga_2O_3 (~ 7 Å) and HgO (~ 16 Å) respectively^{24,25}. In the case of evaporated Al electrodes, it is likely that oxygen (residual oxygen in the vacuum chamber during evaporation, and/or when exposing the samples to air) can form some oxide (likely Al_2O_3) at the interface as observed by infrared spectroscopy on silane junctions²⁶. The last group, referred to as "both oxidized interfaces" is based on alkyltrichlorosilane SAMs on slightly oxidized silicon substrate, and consists of three types of junctions: $\text{Si/SiO}_2\text{-Si-C}_n\text{H}_{2n+1}\text{//Ga}_2\text{O}_3\text{/eGaIn}$, $\text{Si/SiO}_2\text{-Si-C}_n\text{H}_{2n+1}\text{//HgO/Hg}$ and $\text{Si/SiO}_2\text{-Si-C}_n\text{H}_{2n+1}\text{//Al}_2\text{O}_3\text{/Al}$ ($n = 8, 12$).

2.1 Chemicals and SAM fabrication

For alkylthiol ($\text{CH}_3\text{-(CH}_2\text{)}_{n-1}\text{SH}$ with $n = 4, 6, 8, 12, 14, 16, 18$ from Aldrich) SAMs, we used a Si wafer $\langle 100 \rangle$ n-type single side polished as mechanical substrate. It was cleaned with solvents (acetone and isopropanol VLSI grade from Carlo Erba) under ultrasonic bath and dried under nitrogen flow before deposition by sputtering of 10 nm-thick of titanium and 100 nm-thick of gold on substrate heated at 350°C . Then, the gold-coated substrate was directly immersed in a freshly prepared 3×10^{-3} M solution of the alkylthiol in ethanol for a minimum of 48h. The samples were rinsed in an ultrasonic bath with solvents (acetone followed by isopropanol) before use.

For alkene monolayers ($\text{CH}_2=\text{CH}-(\text{CH}_2)_{n-3}-\text{CH}_3$ with $n = 6, 8, 10$ from Aldrich purity >98%), we used a highly-doped Si substrate as bottom electrode. The Si wafer <111> p-type single side polished (resistivity < 0.01 $\Omega\cdot\text{cm}$) was cleaned by rinsing with solvents and blown dry under a stream of argon. Subsequently, the wafer pieces were immersed in piranha solution (98% H_2SO_4 : 30% H_2O_2 , 2:1, v/v) at 90°C for at least 30 min, rinsed with copious amounts of deionized MilliQ wafer and etched in deoxygenated 40% NH_4F solution for ~15 min. This treatment (immersion in piranha solution, rinsing, and etching in 40% NH_4F solution) was repeated once (*caution: piranha solution is very exothermic and reactive with organics; it should be handled with extreme care*). Alkyl monolayers were formed via thermal hydrosilylation of alkenes.^{27;28;29} The freshly etched piece of Si wafer was immersed in neat deoxygenated alkene under argon and heated at 200°C for 4h (for $n = 18, 14$) (or respectively 150, 100 and 70°C for $n = 10, 8, 6$ in order to reduce the evaporation short-chain alkenes). From XPS measurements, we checked that no silicon oxide peak is detected just after the SAM formation. Samples were immediately stored under glove box filled with nitrogen and electrically characterized less than few days after fabrication.

The alkyltrichlorosilane molecules ($\text{CH}_3-(\text{CH}_2)_{n-1}\text{SiCl}_3$ with $n = 8, 12$ from Aldrich) were chemisorbed on naturally oxidized silicon substrates (1 to 1.5 nm thick SiO_2 as measured by ellipsometry) from a dilute solution (10^{-3} M) in an organic solvent (70/30 % v/v of hexane and carbon tetrachloride) using the method developed by Maoz and Sagiv³⁰ and later improved by other groups³¹. The highly-doped (degenerated) n-type <100> silicon substrates (resistivity of $\sim 10^{-3}$ $\Omega\cdot\text{cm}$) were carefully cleaned by a piranha solution (H_2SO_4 : H_2O_2 2/1 v/v) followed a dry UV-ozone treatment. The cleaned substrates were dipped into the freshly prepared solution during 90-120 minutes. The formation of the SAM is highly sensitive to traces of water. For a

1
2
3 better control and a good reproducibility, we worked in a glove box, maintained under a dry and
4
5 clean nitrogen circulation (relative humidity less than 0.1 ppm). After the SAM formation, the
6
7 samples were rinsed in an ultrasonic bath during 5 min with solvents (chloroform followed by
8
9 isopropanol, VLSI grade from Carlo Erba).
10
11

12
13 For all these monolayers, we measured the thickness (ellipsometry) and the water contact
14
15 angle. These values (see Supporting Information) were compared to literature data such as to
16
17 check that we have fabricated SAMs with a good structural quality (densely compact
18
19 monolayer).
20
21

22 **2.2 Aluminum electrode and micropore junction fabrication**

23

24
25 For the electrical measurements, we formed molecular junctions by evaporating metal
26
27 (aluminum) through a shadow mask (electrode area 10^{-4} cm²). To avoid contaminating of the
28
29 surface during metallization, an ultra-high vacuum (UHV, at 10^{-8} torr) electron-beam
30
31 evaporation system was used. In order to avoid, as much as possible, damage of the SAM during
32
33 deposition a low evaporation rate at 3 Å/s was used to form electrodes with a thickness of 40 nm.
34
35 We get a fabrication yield of 95 % (i.e. percentage of non short-circuited junctions).
36
37
38

39
40 The micropores were fabricated in thermally oxidized (SiO₂ 100 nm thick) <100> silicon with
41
42 a low resistivity ($\sim 10^{-3}$ Ω.cm, n-type). Standard e-beam lithography with 200 nm-thick PMMA
43
44 resist (4% 950K) was used, micropores (diameter of 10 and 100 μm, spaced by 350 μm) were
45
46 etched in the silicon dioxide by reactive ion etching (RIE CHF₃ 20 sccm/ CF₄ 20 sccm, 50 mT,
47
48 80 W during 8 min). After removing the resist (with acetone) and wafer cleaning by UV-ozone
49
50 the alkylsilane SAMs were prepared by the same procedure as detailed before. Then a 100 nm-
51
52 thick aluminum layer was deposit on the wafer at 3 Å/s in an UHV electron-beam evaporation
53
54 system as above. Finally top electrodes were patterned (i.e. isolated from each other) by
55
56
57
58
59
60

1
2
3 scratching the aluminum layer around the measured micropore with a tip controlled by a
4 micromanipulator.
5
6

7 8 **2.3 C-AFM measurement** 9

10 Current-voltage measurements were performed by conducting atomic force microscopy (C-
11 AFM) under a nitrogen flow (Dimension 3100, Veeco), using gold-coated tip (from MikroMasch
12 reference CSC17, 0.15 N/m spring constant). To form the molecular junction, the conducting tip
13 was localized at a stationary contact point on the SAM surface at controlled loading force
14 (around 20 nN, otherwise specified). Current–voltage (I-V) characteristics were acquired and
15 treated with the Nanoscope 5.30R2 software from Veeco Instrument Inc. The I-V characteristics
16 were obtained directly by varying voltage from -1.5V/-2V to +1.5V/+2V (depending on
17 breakdown field supported by the various samples) and reversibly, at different places on the
18 sample, without averaging between successive measurements. Moreover, due to the small
19 contact area (about 10 nm² at 20 nN), the measured current is very low (between 100 nA and few
20 pA) and imposes a limit for the SAM thickness (no more than 12 carbon atoms in general). The
21 voltage was applied on the substrate, the tip being ground (i.e. at the input of current amplifier).
22 However, note that for the sake of comparison with eGaIn, Hg drop, Al electrodes, all I-V curves
23 are presented in the figures of this paper with the voltage applied on the top electrode (i.e voltage
24 scale has been inverted for C-AFM measurements).
25
26
27
28
29
30
31
32
33
34
35
36
37
38
39
40
41
42
43
44

45 46 **2.4 eGaIn and Hg drops contacts** 47

48 To form molecular junctions, we also used eutectic Gallium Indium drop contact (eGaIn
49 99.99%, Ga:In; 75.5:24.5 wt% from Alfa Aesar). We used a method close to the one developed
50 by Chiechi *et al.*³². We formed a drop of eGaIn at the extremity of a needle fixed on a
51 micromanipulator. By displacing the needle, we brought the drop into contact with a sacrificial
52
53
54
55
56
57
58
59
60

surface, and we retracted the needle slowly. By this technique, we formed a conical tip of eGaIn with a diameter of around 200 μm (corresponding to contact area of $\sim 10^{-3} \text{ cm}^2$). This conical tip was then put into contact with the SAM (under control with a digital video camera). We used the eGaIn tip at different places on the samples and we regularly formed a new tip for a same sample to avoid pollution of the tip. The eutectic GaIn drop allows a good electric contact with the SAM since eGaIn accommodates well the surface roughness, and can be used on gold without forming amalgam.³²

We also used a hanging mercury drop, to contact the SAM. Calibrated mercury drops (99.9999%, purchased from Fluka) were generated by a controlled growth mercury electrode system (CGME model from BASi). The mechanical contact between the sample and the hanging mercury drop was formed by moving up a precision lab-lift (supporting the sample) under the control of a digital video camera. The electrical contact area estimated by capacitance measurement is around 10^{-4} cm^2 . This technique is only used for SAMs on Si substrates.

2.5 I-V and TVS measurement protocol

For eGaIn, Hg drop, micropore and aluminum pads, the current-voltage measurements were done with an Agilent 4156C parameter analyzer, the voltage was always applied on the top electrode and the current measured at the grounded substrate. As for C-AFM, voltage was varied from -1.5 V to +1.5 V and reversibly from +1.5 V to -1.5 V, at different places on the sample, without any averaging between successive measurements. Five to more than 30 I-V were measured for each junctions made with the different molecules, top contacts and chain length. This number is sample dependent and depends on the removal of I-V curves characterized by the presence of short-circuits (very large current density $> 1 \text{ A/cm}^2$) or poor electrical contact (i.e. with large noise or sudden and random step-like current fluctuations). Voltages at which a

1
2
3 minimum in the $\ln(I/V^2)$ vs. $1/V$ were determined for each measurement and averaged to give the
4
5 transition voltages for positive bias (V_{T+}) and for negative bias (V_{T-}) as well as the standard
6
7 deviation (reported as the error bars in the figures) for each kind of junctions. For samples with a
8
9 number of I-V measurements smaller than 10, we simply used the average value, for samples
10
11 with a larger number of data (C-AFM), we plotted V_T histograms, which were fitted by a
12
13 Gaussian distribution.
14
15

16 17 18 3. RESULTS AND DISCUSSIONS

19 20 3.1. Oxide-free junctions: Alkylthiol on Au and Alkene on Si measured by C-AFM

21
22 We measured current-voltage (I-V) curves for oxide free junctions with the following
23
24 structure: freshly evaporated gold substrate/SAM/gold covered AFM-tip (see Experimental
25
26 Methods). A typical set of 19 I-V curves for the $\text{Au}_{\text{sub}}\text{-S-C}_n\text{H}_{2n+1}\text{//Au}_{\text{tip}}$ ($n=4$) is shown in Fig. 2-
27
28 a, and the corresponding $\ln(I/V^2)$ vs. $1/V$ in Fig. 2-b. Fig. 2-c shows the V_T histograms obtained
29
30 from Fig. 2-b, from which we get the V_{T+} and V_{T-} (and standard deviation) values for this
31
32 junction (see experimental methods). The V_{T+} and V_{T-} values for junctions made of alkylthiols
33
34 with different chain length ($\text{Au}_{\text{sub}}\text{-S-C}_n\text{H}_{2n+1}\text{//Au}_{\text{tip}}$) are presented in figure 3. The values for V_{T+}
35
36 and V_{T-} are independent of the alkylthiol chain length in the SAM ($n=4$ to 12). Note that for
37
38 $n>12$ (for the alkylthiol), no current can be measured due to the small contact area of the C-AFM
39
40 tip. These V_{T+} values are in good agreement with Beebe *et al.*⁴, who reported values between
41
42 1.20 ± 0.08 V and 1.28 ± 0.12 V, measured on the same kind of junctions (n from 6 to 12) with
43
44 the C-AFM technique.
45
46
47
48
49

50
51 Albeit TVS measurements for both bias polarity are sparsely reported, V_T should strongly
52
53 depend on the bias polarity due to the asymmetry of the junction, especially if the two
54
55 electrode/organic interfaces are different.^{3;4;33;34} These asymmetric junctions present unequal
56
57
58
59
60

voltage drop at the two interfaces inducing a difference between the absolute values of V_{T+} and V_{T-} . This feature was supported by *ab initio* DFT transport calculations simulating TVS curves for various molecular junctions²³.

Here, we systematically measured TVS for both bias polarities, in order to figure out if there is a general trend relating the structure (symmetric vs. asymmetric) of the junctions and the ratio V_{T+}/V_{T-} . The V_{T+} and V_{T-} values are shown in Fig. 3 and Table 1. Considering the error bars, the measured transition voltages are equal in absolute values for both polarities. For alkylthiol junctions, the averaged values of the transition voltages measured for each chain lengths are $V_{T+ave} = 1.32 \pm 0.08$ V and $V_{T-ave} = -1.26 \pm 0.08$ V (table 1), thus a TVS asymmetry ratio:

$$TVS-AR = \max\left(\left|\frac{V_{T+}}{V_{T-}}\right|, \left|\frac{V_{T-}}{V_{T+}}\right|\right) \quad (1)$$

is of about 1.06 ± 0.13 . Other authors³⁵ measured TVS on molecular junctions with nonanedithiol and decanedithiol SAMs. The V_{T+} values are the same for both molecules, about 1.1 ± 0.07 V. Recently, values in the range 1.1 - 1.5 V were reported for 8 and 10 carbon atoms alkylthiol single molecule using STM based break junction methods, irrespective to the bias polarity, i.e. with a TVS-AR between 1 and 1.2¹³. Albeit the test-bed structures are not the same, and thus both the position of the molecular orbitals and the electronic coupling with electrodes can change from experiment to experiment, all these experiments show that the transition voltages are in the same range, with a rather symmetrical behavior for both bias polarities.

The loading force applied on the C-AFM tip is an important parameter when measuring the transport properties of SAM junctions. In general, the loading force is chosen arbitrary between few nN and few tens of nN.^{3;4} However, the loading force affects radically the current^{17;36;37} which increases with the loading force (e.g. the current measured on C8 alkylthiol is multiplied by more than 10^2 when the force increases from 2 to 10 nN)³⁶. We checked the effect of the

loading force from 10 nN to 40 nN on V_T for alkylthiol ($n=12$) junctions (Figure 4). In this force range, we do not observe any influence. The V_T values are almost constant for both bias polarities, with averaged values of $V_{T+ave} = 1.23 \pm 0.03$ V and $V_{T-ave} = -1.25 \pm 0.06$ V. Wang *et al.*³⁴ report a decrease of the transition voltage in the range 50 - 100 nN, which is attributed to a disorder-induced enhancement of the electronic transport (i.e. enhancement of the intermolecular chain-to-chain tunneling when increasing the molecule tilt by the applied force). Such a disorder related effect is not important here with loading forces smaller than 40 nN.

Figure 5 and table 1 show the TVS results for the Si-C_nH_{2n+1}//Au_{tip} junctions. Again, we measured V_T values independent of the chain length (above $n=10$, the current is too low to be measured by C-AFM). The average value is $V_{T-ave} = -0.96 \pm 0.15$ V. Note that we have not observed a transition voltage for the positive bias (except for $n=8$). This feature may be due to the fact that the measured current was too low for the positive bias, because these Si-C_nH_{2n+1}//Au_{tip} junctions are more asymmetric than the alkylthiol one. This is confirmed by the larger (in absolute value) V_{T+} of 1.4 V measured for the $n=8$ junction (TVS-AR ≈ 1.4).

3.2. Junctions with oxidized top electrode: Alkylthiol with eGaIn top contact, and Alkene with Hg, eGaIn or Al top electrode

We also characterized the same SAMs using eGaIn drop contact to compare the effect of the top electrode on V_T values. The eGaIn drop presents on the surface a thin layer (*ca.* 0.7 nm) of gallium oxide (mainly Ga₂O₃) that contains many defects.²⁴ It is usually assumed that these defects may dope the oxide layer making it highly conducting. For this reason, the influence of this layer on the electrical properties of the molecular junctions is usually neglected.^{24;38} For instance, Reus *et al.*³⁸ demonstrated that rectifying behavior in molecular junctions (ferrocene and naphthoquinone derivatives) are due to the electronic properties of the SAM and not to the

presence of Ga_2O_3 layer.³⁸ However, TVS data were not reported for these systems. Alkene monolayers on silicon were also characterized using a mercury drop and an aluminum electrode deposited by evaporation through a shadow mask. These materials present also a thin surface layer of oxide that forms when the metal is exposed to air, respectively HgO and Al_2O_3 (in this latter case, it is likely that Al_2O_3 is not only formed at the outer surface of Al, but also at the Al/monolayer interface, since O may diffuse through the organic SAM). These later two approaches cannot be applied for SAM on gold because mercury forms spontaneously amalgam with gold through the single monolayer (capping the Hg/HgO drop with a second SAM may be used to delay the amalgam formation,³⁹ but was not used here), and aluminum evaporated on SAM on Au causes 100% short circuited devices.

From the current-voltage characteristics measured with the eutectic GaIn drop on a series of alkylthiol $\text{Au}_{\text{sub}}\text{-S-C}_n\text{H}_{2n+1}/\text{Ga}_2\text{O}_3/\text{eGaIn}$ junctions (4 to 18 carbon atoms) two V_T values are deduced, one for each polarities, which are independent of the length of molecules (Fig. 3, table 1) as already observed above by C-AFM and by other groups.^{3,6} The average value determined for all the $\text{Au}_{\text{sub}}\text{-S-C}_n\text{H}_{2n+1}/\text{Ga}_2\text{O}_3/\text{eGaIn}$ junctions at positive and negative bias are respectively $V_{T+\text{ave}} = 0.44 \pm 0.12$ V and $V_{T-\text{ave}} = -0.52 \pm 0.06$ V. Considering uncertainties, V_T values are equal (in absolute values) for both polarities as observed by C-AFM.

In figure 3, the comparison between eGaIn and C-AFM measurements shows the influence of the top electrode on the V_T values. By changing the top electrode from gold (C-AFM) to oxidized GaIn (eGaIn/ Ga_2O_3) the V_T value decreases by *ca.* 0.8 - 0.9 V. The origin of this decrease can be due to two factors: (i) the reduction of the work function of *ca.* 1eV from gold to eGaIn,^{19;24} (ii) or the presence of oxides states related to the Ga_2O_3 layer in the junction. In the first case, a reduction (in absolute value) of both V_{T+} and V_{T-} with a decrease of the work

function implies that the tunneling transport is LUMO-mediated (see discussion section) with a nearly ideal symmetric junction (i.e. $\gamma = 0$, where γ is a voltage division parameter describing the degree of symmetry or asymmetry of the molecular orbitals in the junction, $-0.5 \leq \gamma \leq 0.5$).^{10;11} Albeit there is no data in literature for γ in the case of molecular junction with eGaIn electrodes, DFT calculations predicted an almost symmetric coupling ($\gamma = 0.14 - 0.16$) for the $\text{Au}_{\text{sub}}\text{-S-C}_n\text{H}_{2n+1}\text{//Au}_{\text{tip}}$ junctions.¹⁰ In the second case, we assume that oxide states are introduced at energy smaller than the LUMO/HOMO gap, and that these states are now probed by the TVS method at lower bias than for the molecular orbitals. This point will be further discussed below (see discussion section).

In the case of alkene molecules directly grafted on silicon without native oxide and electrically contacted by top oxidized electrodes (mercury drop contact, eGaIn drop or aluminum patterns), I-V curves plotted in TVS form show clear and reproducible minima. The V_T values for the three junctions, $\text{Si-C}_n\text{H}_{2n+1}\text{//Ga}_2\text{O}_3\text{/eGaIn}$, $\text{Si-C}_n\text{H}_{2n+1}\text{//HgO/Hg}$ and $\text{Si-C}_n\text{H}_{2n+1}\text{/Al}_2\text{O}_3\text{/Al}$, are reported Fig. 5 and in table 1 for comparison with the $\text{Si-C}_n\text{H}_{2n+1}\text{//Au}_{\text{tip}}$ C-AFM junction. Again, the V_T values are almost independent of the molecule length (if we except a slight increase for $n = 14$ and 18 in the case of the eGaIn contacts, but with a large data dispersion). Also, the V_T values are almost symmetric for both polarities. We note that these values for the different junctions with the different top electrodes are quite similar. The fact that V_T values are almost the same whatever the nature of the oxidized electrodes (averaged values of $V_{T+\text{ave}} = 0.27 \pm 0.14$ V and $V_{T-\text{ave}} = -0.37 \pm 0.18$ V for positive and negative bias, horizontal lines in Fig. 5) supports the hypothesis that TVS is measuring some oxide states in the junctions lying inside the LUMO/HOMO gap.

3.3. Junctions with both oxidized interface: alkyltrichlorosilane

Alkyltrichlorosilane SAMs grafted on slightly oxidized silicon were used to fabricate molecular junctions with two oxidized interfaces. Different electrodes were used to electrically characterized these junctions, all with oxidized metals (eGaIn, Hg and Al): Si/SiO₂-Si-C_nH_{2n+1}//Ga₂O₃/eGaIn, Si/SiO₂-Si-C_nH_{2n+1}//HgO/Hg and Si/SiO₂-Si-C_nH_{2n+1}//Al₂O₃/Al (n=8, 12). The presence of both a silicon oxide and the SAM does not allow using C-AFM, the current is too low. Again, V_T values are independent of chain length, bias polarity, and size of the surface contact area (from 10⁻³ cm² to 10⁻⁶ cm² for respectively Hg, eGaIn drops and 10 μm and 100 μm diameter micropores) as summarized in Fig. 6 and Table 1. The V_T values for all these alkyltrichlorosilane junctions are close to the previous values obtained on alkene SAMs with a top oxidized contact (see Fig. 5), with average values of V_{T+ave} = 0.25 ± 0.10 V and V_{T-ave} = -0.21 ± 0.08 V respectively for positive and negative bias (horizontal lines Figure 6). For Si/SiO₂-Si-C_nH_{2n+1}//Al₂O₃/Al junctions, LUMO and HOMO energy levels with respect to the Fermi energy of the electrodes were reported at ~ 4 - 4.5 eV by photoconductivity experiments.^{21;40} Thus, we expect V_T to be in the range of a few eV in that case. This major discrepancy between the V_T and the barrier height estimated by another way shows the limitation of the TVS approach for these oxidized junctions. This is corroborated by V_T measured on a reference junction (*i.e.* without SAM; aluminum, eGaIn or mercury directly deposited on silicon with its native oxide), as reported in figure 6 and in table 1 as n=0. The same V_T values are measured with and without the SAM. Thus, it is likely that these low V_T values correspond to oxide-related states located close to the electrode Fermi energy rather than related to the HOMO or LUMO of the molecules.

4. DISCUSSION

For the interpretation of these TVS results, we follow Araidi and Tsukada¹² who suggested, on the basis of non-equilibrium Green's function combined with both density-functional theory and

tight-binding approximation, that the TVS transition voltage corresponds to the bias situation when the tail of the density of states (DoS) of the molecular orbitals (HOMO or LUMO) enters the energy window defined by the applied bias (see figure 7.a). We also assume that electron transport properties is controlled by the LUMO as recently demonstrated for both alkylthiol junctions on Au⁴¹ and alkene on hydrogenated silicon.⁴² Inverse photoemission spectroscopy (IPES) on C18/Au interface shows that the LUMO-edge is at 3.35 eV above the Au Fermi energy⁴¹, far away the transition voltage of about 1.2 - 1.3 V. However, a clear DoS tail is also observed at lower energy, which is related to induced-density of interface states (IDIS) or metal-induced gap states (MIGS).^{43;44;45} These states are due to hybridization between the molecule and metal (electrode generally speaking) states. Thus, we assume that the transition voltage arises when a certain amount of these states enter the energy window. Recent discussions in the literature point out how it can be possible to relate V_{T+} and V_{T-} to the energy position of the LUMO or HOMO levels in the junctions and to the voltage division factor γ , a parameter that describes the degree of symmetry or asymmetry of the molecular orbitals in the junction ($-0.5 \leq \gamma \leq 0.5$, $\gamma = 0$ being the case of a symmetrical coupling of the molecular orbitals between the two electrodes).^{9;10;11;23} Following the analytical model of Bâldea,¹¹ we determine the energy level ε_0 of the molecular orbital involved (here LUMO) in the electrical transport (with respect to the Fermi energy of the electrodes), and γ , directly from the measured V_{T+} and V_{T-} according to:

$$\begin{aligned} |\varepsilon_0| &= 2 \frac{e|V_{T+}V_{T-}|}{\sqrt{V_{T+}^2 + 10|V_{T+}V_{T-}|/3 + V_{T-}^2}} \\ \gamma &= \frac{\text{sign } \varepsilon_0}{2} \frac{V_{T+} + V_{T-}}{\sqrt{V_{T+}^2 + 10|V_{T+}V_{T-}|/3 + V_{T-}^2}} \end{aligned} \quad (2)$$

where $\text{sign } \varepsilon_0$ is + for LUMO (- for HOMO). For the Au_{sub}-S-C_nH_{2n+1}//Au_{tip} junction, we get $\varepsilon_0 = 1.12 \pm 0.10$ eV, and $\gamma \approx 0$ (see Table 1). This energy level is in very good agreement with the

onset of the LUMO tail in this junction as measured by IPES⁴¹ (starting very close to the metal Fermi energy, see Fig. 4 in ref. 36).

For the Si-C_nH_{2n+1}//Au_{tip} junctions, the same approach for n=8 gives $\epsilon_0 = 1.03 \pm 0.63$ eV, and $\gamma \approx 0.068$. IPES shows the LUMO edge at about 3.1 eV above the Si Fermi energy⁴² but again with a clear DoS tail starting at about 1 eV^{42;46} in very good agreement with this value of ϵ_0 . We have to note that this comparison is meaningful because our samples were fabricated strictly following the same process as the one developed by the authors of refs 42 and 46.

Also note that IPES measurements²² were carried out on long chains (16 and 18 carbon atoms) while our TVS experiments are carried out on smaller chains (n= 4 - 12). However, this is not (both experimentally and theoretically) that there is no dependence of the LUMO/HOMO gap, nor LUMO position, as function of the number of carbon atoms in the chain (at least for n larger than 4).^{4;6;21;22;33} In case of π -conjugated molecules of different chemical nature measured by C-AFM ("clean junction"), Beebe et al. have shown that V_T is linearly dependent on the position of the HOMO.^{3;4} For all the other junctions, with one or two oxidized electrodes, we suppose that the lower values of V_T ($|V_T| < 0.6$ eV) are due to some oxide states as schematically shown in Fig. 7b. The role of these states in the electronic conduction of molecular junctions was already suggested,⁴⁷ and theoretically taken into account very recently to explain some discrepancies between experiments and TVS models.⁴⁸ Here, the role of these oxide states is confirmed by TVS measurement with C-AFM on a reference sample without SAM, i.e. a slightly oxidized silicon (~ 7.5 Å of SiO₂ on n-type <100> silicon, resistivity of 10^{-3} Ω.cm). We also measured low values, $V_{T+} = 0.09 \pm 0.05$ V and $V_{T-} = -0.14 \pm 0.06$ V, i.e in the same range as for any other SAM junctions with oxidized electrodes. Oxide states near the Si Fermi energy have also been observed in metal-oxide-semiconductor devices, leading to low tunneling barrier heights.⁴⁹ Note

1
2
3 that low V_T values (around 0.2 V) have also been reported for other molecular junctions on Si
4
5 (using acid terminated alkylthiol) and ascribed to the formation of interface states at the
6
7 Si/molecule interface.^{15,16}
8
9

10 **5. CONCLUSION**

11
12 To conclude, we have electrically characterized by TVS method a large number of various
13
14 molecular junctions made with alkyl chains but with different chemical structure of the
15
16 electrode/molecule interfaces. In the case of molecular junctions with “clean, unoxidized”
17
18 electrode/molecule interfaces, we conclude that the TVS method allows estimating the onset of
19
20 the tail of the LUMO density of states when alkylthiols and alkenes are grafted on Au and
21
22 hydrogenated Si, respectively, with $|V_T|$ in the range of 0.9-1.4 V. Otherwise, in the case of
23
24 “oxidized” interfaces (e.g. the same monolayer measured with Hg or eGaIn drops, or monolayers
25
26 on a slightly oxidized silicon substrate), lower $|V_T|$ (0.2-0.6V) are systematically measured and
27
28 related to the presence of oxide-related density of states at lower energies than the
29
30 HOMO/LUMO of the molecules. As such, the TVS method is a useful technique to assess the
31
32 quality of the molecule/electrode interfaces in molecular junctions.
33
34
35
36
37
38
39
40
41
42
43
44
45
46
47
48
49
50
51
52
53
54
55
56
57
58
59
60

Junction	top contact	n	V_{T+} (V)	V_{T-} (V)	$ \epsilon_0 $ (eV)	γ
Au _{sub} -S-C _n H _{2n+1}	C-AFM	4	1.40±0.24	-1.29±0.17	1.16±0.25	-0.018
		6	1.34±0.10	-1.33±0.36	1.16±0.33	-0.002
		8	1.21±0.13	-1.17±0.13	1.03±0.16	-0.007
		12	1.33±0.04	-1.23±0.11	1.11±0.10	-0.017
		average	1.32±0.08	-1.26±0.07	1.12±0.10	-0.010
Si-C _n H _{2n+1}	C-AFM	6		-0.86±0.23	--	--
		8	1.4±0.84	-1.02±0.12	1.03±0.63	-0.068
		10		-1.00±0.10	--	--
		average	NS	-0.96±0.09	--	--
Au _{sub} -S-C _n H _{2n+1}	eGaIn	4	0.32±0.34	-0.42±0.14	0.32±0.36	0.059
		6	0.43±0.31	-0.59±0.04	0.43±0.31	0.068
		8	0.36±0.27	-0.48±0.04	0.36±0.27	0.062
		12	0.47±0.09	-0.52±0.25	0.43±0.22	0.022
		14	0.45±0.07	-0.52±0.07	0.42±0.09	0.031
		16	0.37±0.33	-0.58±0.12	0.39±0.36	0.096
		18	0.69±0.33	-0.52±0.25	0.51±0.35	-0.061
		average	0.44±0.12	-0.52±0.06	0.41±0.12	0.036
Si-C _n H _{2n+1}	Hg drop	10	0.17±0.12	-0.43±0.05	0.22±0.16	0.192
		14	0.19±0.06	-0.19±0.06	0.16±0.07	0.000
		18	0.20±0.05	-0.25±0.07	0.19±0.07	0.048
	eGaIn	6	0.14±0.01	-0.18±0.05	0.14±0.04	0.054
		8	0.23±0.11	-0.39±0.05	0.25±0.12	0.113
		10	0.23±0.05	-0.14±0.04	0.15±0.05	-0.106
		14	0.57±0.29	-0.64±0.26	0.52±0.34	0.025
		18	0.50±0.48	-0.41±0.26	0.39±0.45	-0.043
	Al pad	10	0.19±0.01	-0.57±0.07	0.25±0.03	0.224
		14	0.25±0.04	-0.62±0.04	0.31±0.05	0.188
		18	0.27±0.22	-0.29±0.19	0.24±0.25	0.015
		average	0.27±0.14	-0.37±0.18	0.27±0.20	0.068
Si/SiO ₂ -Si-C _n H _{2n+1}	Hg drop	8	0.16±0.05	-0.16±0.05	0.14±0.06	0.000
		12	0.16±0.05	-0.16±0.05	0.14±0.06	0.000
	Al pads	8	0.16±0.05	-0.12±0.01	0.12±0.04	-0.062
		12	0.35±0.31	-0.19±0.02	0.22±0.20	-0.130
	μpore 10μm	8	0.27±0.09	-0.37±0.27	0.27±0.22	0.068
		12	0.33±0.08	-0.28±0.08	0.26±0.10	-0.036
	μpore 100μm	8	0.17±0.02	-0.18±0.06	0.15±0.05	0.012
		12	0.17±0.02	-0.19±0.05	0.16±0.04	0.024

	eGaIn	8	0.30±0.04	-0.18±0.06	0.20±0.05	-0.11
		12	0.43±0.19	-0.19±0.05	0.23±0.04	-0.17
		average	0.25±0.10	-0.21±0.08	0.20±0.11	-0.038
Reference sample	eGaIn	0	0.24±0.02	-0.23±0.05	0.20±0.05	-0.009
	Micropore	0	0.19±0.05	-0.23±0.06	0.18±0.07	0.041
	Hg drop	0	0.24±0.05	-0.13±0.01	0.15±0.03	-0.130

Table 1. Summary of the measured V_{T+} and V_{T-} for all the junctions investigated in this work (n is the number of carbon atoms in the alkyl chain). NS means “not significant”. Energy level ϵ_0 and asymmetry factor γ deduced from eqs. (2) for all the measured junctions.

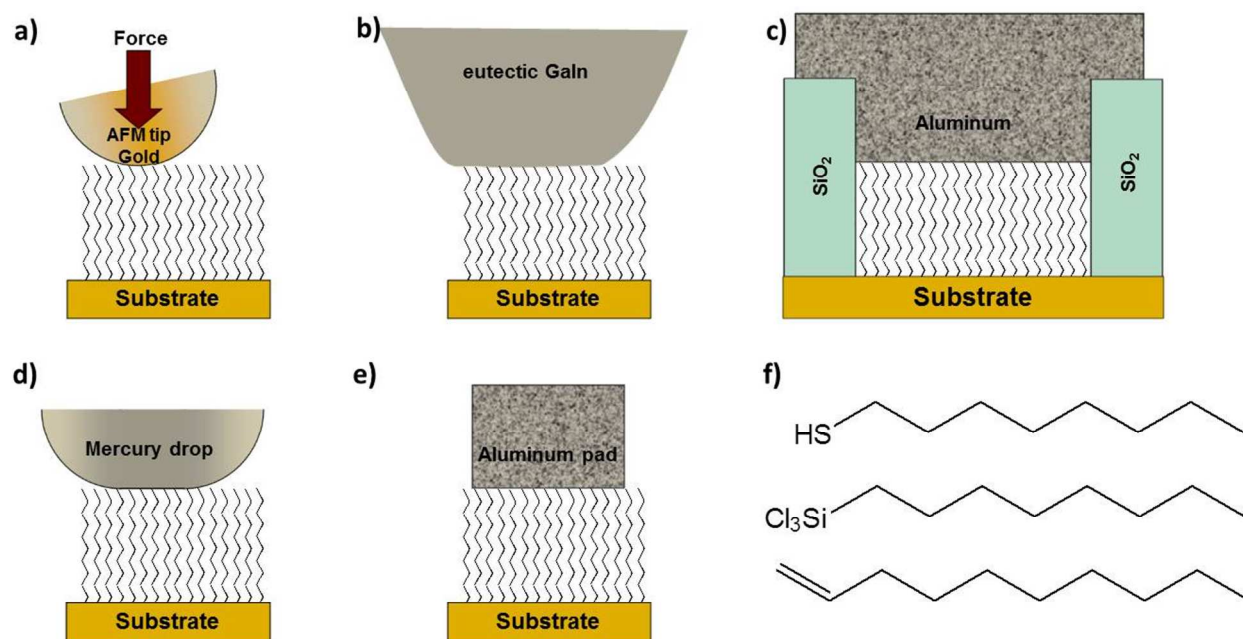


Figure 1. Schematic representation of the different molecular junctions. The substrate is gold, hydrogenated silicon or natively oxidized silicon. The top electrode is: a) a conducting-AFM with gold tip, b) an eutectic GaIn drop, c) an evaporated Al electrode on a SAM grafted in a micropore junction fabricated in SiO₂ by conventional lithography, d) a mercury drop, e) an evaporated aluminum pads through a shadow mask. f) the three families of alkyl molecules (from top to bottom): alkylthiol ($\text{CH}_3-(\text{CH}_2)_{n-1}\text{SH}$ with $n=4;6;8;12;14;16;18$), alkyltrichlorosilane ($\text{CH}_3-(\text{CH}_2)_{n-1}\text{SiCl}_3$) with $n=8; 12$) and alkene ($\text{CH}_2=\text{CH}-(\text{CH}_2)_{n-3}-\text{CH}_3$ with $n=6; 8; 10$).

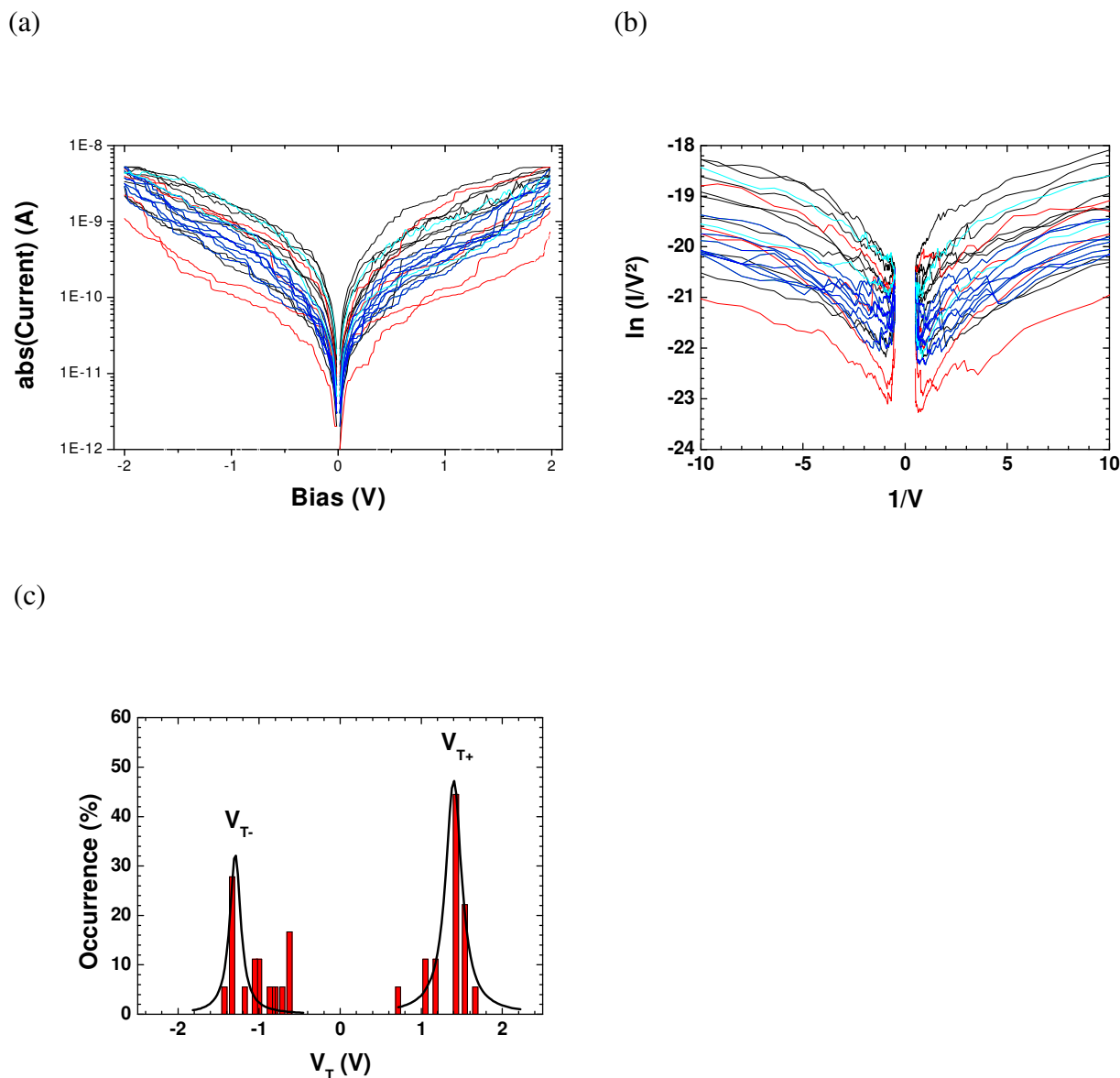


Figure 2: Example for the junction $\text{Au}_{\text{sub}}\text{-S-C}_n\text{H}_{2n+1}/\text{Au}_{\text{tip}}$ with $n=4$ of (a) the set of 19 I-V curves measured on this junction; (b) the Fowler-Nordheim plots obtained from these I-V curves and (c) V_T histograms obtained from the Fowler-Nordheim plots, from which we get the V_{T+} , V_{T-} and standard deviation values presented in table 1 (black line is the Gaussian fit).

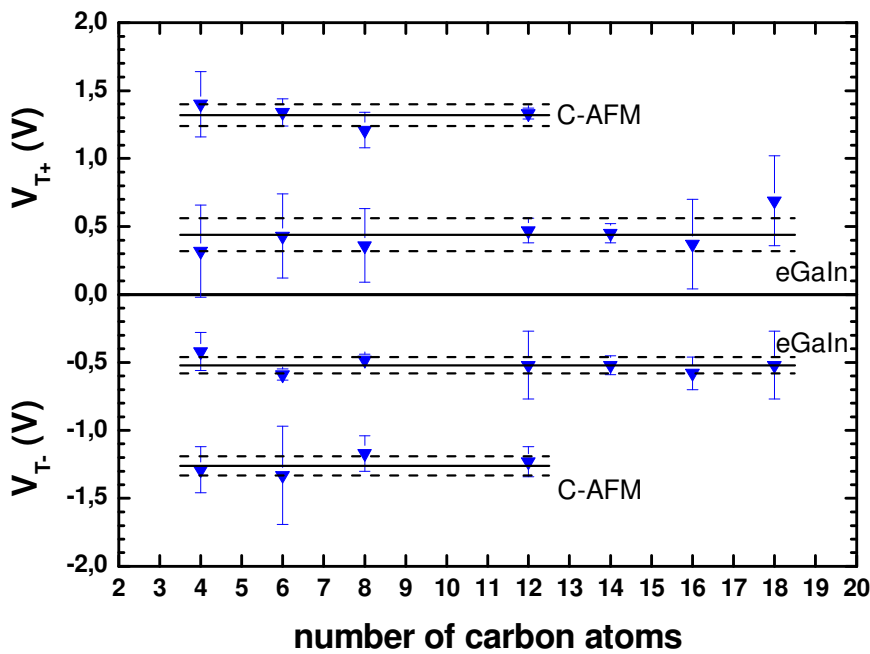


Figure 3. V_{T+} and V_{T-} values for alkylthiol SAMs determined from 5 to 20 I-V curves by C-AFM at ca. 20nN and by eGaIn contact, as function of the length of the alkyl chain. The solid lines correspond to the average value for V_T , and the dashed lines are the standard deviation. These average values for V_{T+} and V_{T-} determined for this set of junctions by C-AFM and by eGaIn drop are respectively $V_{T+ave} = 1.32 \pm 0.08$ V; $V_{T-ave} = -1.26 \pm 0.07$ V and $V_{T+ave} = 0.44 \pm 0.12$ V; $V_{T-ave} = -0.52 \pm 0.06$ V.

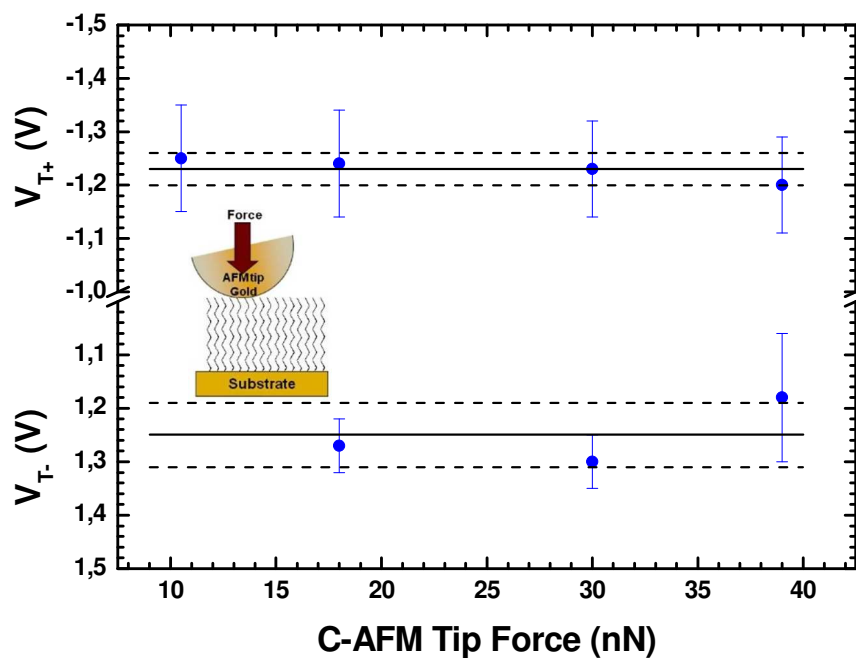


Figure 4: V_{T+} and V_{T-} determined from 5 I-V curves for the $\text{Au}_{\text{sub}}\text{-S-C}_n\text{H}_{2n+1}$ ($n=12$) junction as function of the loading force on the AFM tip. The solid lines correspond to the average value for V_{T-} , and the dashed lines the standard deviation.

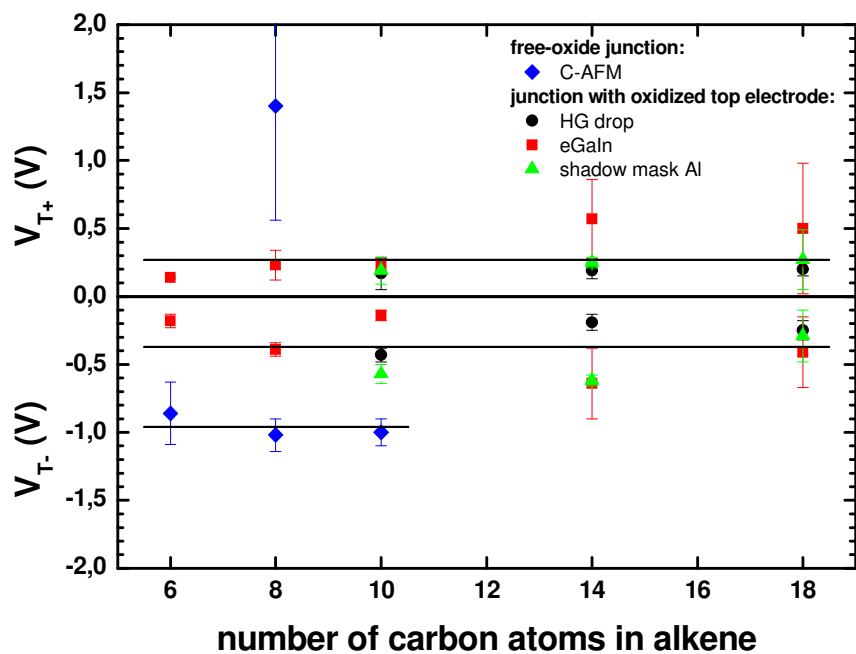


Fig. 5: V_{T+} and V_{T-} determined for the Si- C_nH_{2n+1} junctions in the case of oxide-free junction (C-AFM top electrode) and for junctions with oxidized top electrode (mercury drop, eGaIn drop and aluminum patterns). Each point corresponds to an average on 5-18 I-V curves, and the error-bar to the standard deviation. For negative bias, two families of measurements are clearly distinguishable: for “clean junctions” with an averaged $V_{T-ave} = -0.96 \pm 0.09$ V, and for “oxidized junction” $V_{T-ave} = -0.37 \pm 0.18$ V and $V_{T+ave} = 0.27 \pm 0.20$ V as indicated by horizontal solid lines.

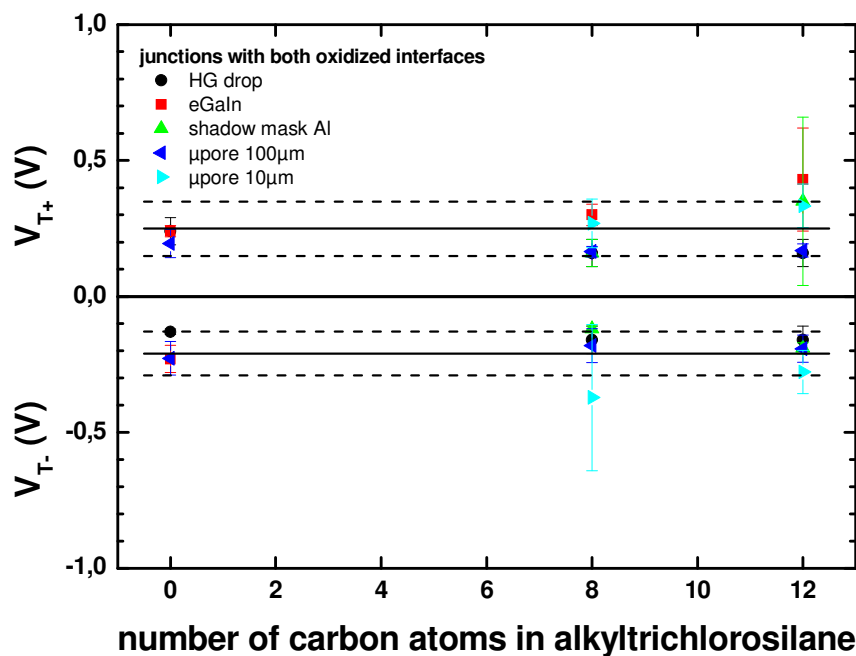
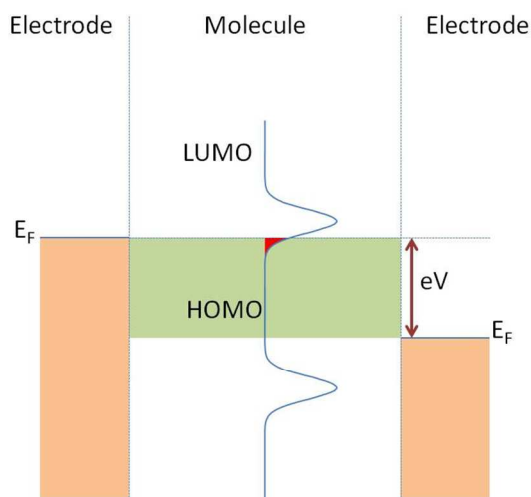


Figure 6: V_{T+} and V_{T-} determined for the Si/SiO₂-Si-C_nH_{2n+1} junctions in the case of both oxidized interfaces: silicon with ca. 1.3nm-thick silicon dioxide and oxidized top electrode (mercury drop, eGaIn drop and aluminum patterns). Each point corresponds to an average on 5-28 I-V curves, and the error bar to the standard deviation. Whatever the nature of the metal top electrode, V_T values are quite similar. Averaging over the different lengths and type of top electrodes gives: $V_{T+ave} = 0.25 \pm 0.10$ V, and $V_{T-ave} = -0.21 \pm 0.08$ V as shown by horizontal solid lines in the graph, the dashed lines being the standard deviation.

(a)



(b)

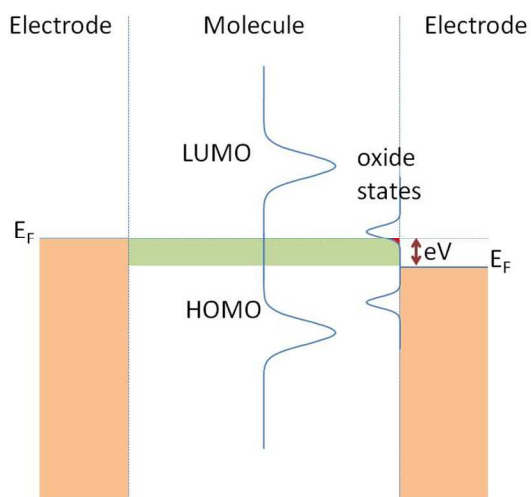


Figure 7. Schematic representations of the energy level diagrams at the threshold point of the TVS plot curve (*i.e.* when the applied bias is close to V_T) for (a) an oxide-free clean and (b) a junction with an oxidized electrode. The two electrodes are represented by the Fermi energies, the molecule by the HOMO and LUMO energies, and the oxide by energy bands close to the Fermi energy of the oxidized electrode.

ASSOCIATED CONTENT

Supporting information. Ellipsometry and water contact angle measurements are available free of charge via the Internet at <http://pubs.acs.org>.

AUTHOR INFORMATION

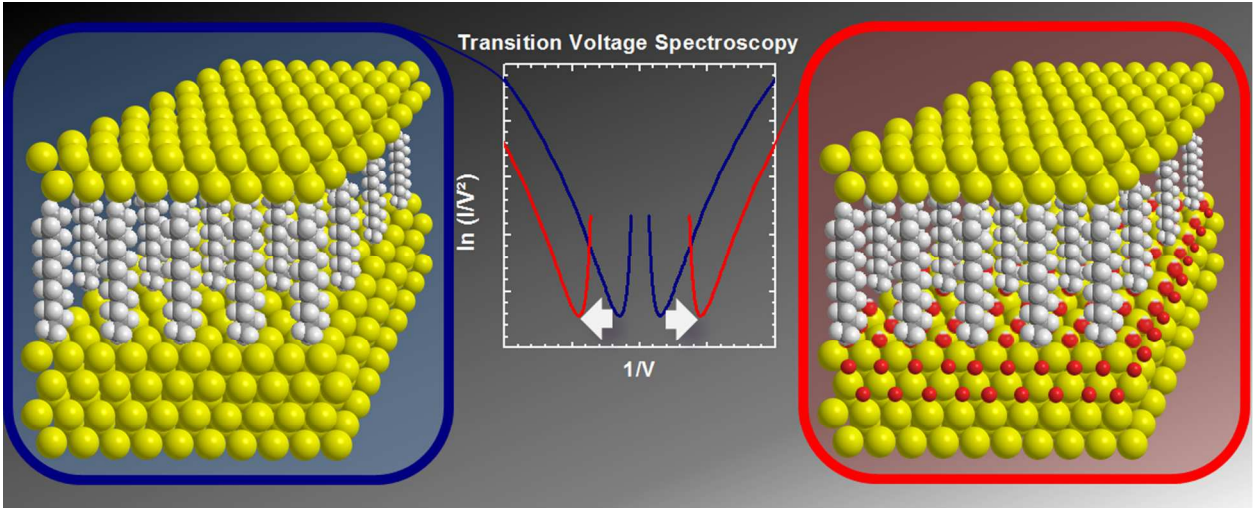
Corresponding Author

* E-mail: dominique.vuillaume@iemn.univ-lille1.fr; stephane.lenfant@iemn.univ-lille1.fr

ACKNOWLEDGMENT

G.R. thanks the CNRS and the Région Nord-Pas de Calais for the PhD grant funding (contract number 72837). We thank Nicolas Clément and Stéphane Pleutin for fruitful discussions, Dominique Deresmes for assistance in C-AFM, and the clean room staff for the assistance and guidance for micropore fabrication.

TOC GRAPHIC



REFERENCES

- 1 McCreery, R. L.; Bergren, A. J., *Advanced Materials* **2009**, *21* (43), 4303-4322.
- 2 Salomon, A.; Cahen, D.; Lindsay, S. M.; Tomfohr, J.; Engelkes, V. B.; Frisbie, C. D.,
3 *Adv. Mat.* **2003**, *15* (22), 1881-1890.
- 4 Beebe, J. M.; Kim, B.; Frisbie, C. D.; Kushmerick, J. G., *ACS Nano* **2008**, *2* (5), 827-832.
- 5 Beebe, J. M.; Kim, B.; Gadzuk, J. W.; Frisbie, C. D.; Kushmerick, J. G., *Physical Review*
6 *Letters* **2006**, *97* (2), 026801.
- 7 Bennett, N.; Xu, G.; Esdaile, L. J.; Anderson, H. L.; Macdonald, J. E.; Elliott, M., *Small*
8 **2010**, *6* (22), 2604-2611.
- 9 Song, H.; Kim, Y.; Jeong, H.; Reed, M. A.; Lee, T., *The Journal of Physical Chemistry C*
10 **2010**, *114* (48), 20431-20435..
- 11 Lu, Q.; Liu, K.; Zhang, H.; Du, Z.; Wang, X.; Wang, F., *ACS Nano* **2009**, *3* (12), 3861-
12 3868.
- 13 Simmons, J. G., *J. Appl. Phys.* **1963**, *34* (6), 1793-1803.
- 14 Huisman, E. H.; Guédon, C. M.; van Wees, B. J.; van der Molen, S. J., *Nano Letters*
15 **2009**, *9* (11), 3909-3913.
- 16 Chen, J.; Markussen, T.; Thygesen, K. S., *Physical Review B* **2010**, *82* (12), 121412.
- 17 Bâldea, I., *Ibid.* **2012**, *85* (3), 035442.
- 18 Araidai, M.; Tsukada, M., *Ibid.* **2010**, *81* (23), 235114.

-
- 13 Guo, S.; Hihath, J.; Díez-Pérez, I.; Tao, N., *Journal of the American Chemical Society* **2011**, *133* (47), 19189-19197.
- 14 Clément, N.; Patriarche, G.; Smaali, K.; Vaurette, F.; Nishiguchi, K.; Troadec, D.; Fujiwara, A.; Vuillaume, D., *Small* **2011**, *7* (18), 2607-2613.
- 15 Yu, L. H.; Gergel-Hackett, N.; Zangmeister, C. D.; Hacker, C. A.; Richter, C. A.; Kushmerick, J. G., *J. Phys.: Condens. Matter* **2008**, *20* (37), 374114.
- 16 Coll, M.; Miller, L. H.; Richter, L. J.; Hines, D. R.; Jurchescu, O. D.; Gergel-Hackett, N.; Richter, C. A.; Hacker, C. A., *Journal of the American Chemical Society* **2009**, *131* (34), 12451-12457.
- 17 Wold, D. J.; Frisbie, C. D., *J. Am. Chem. Soc.* **2001**, *123*, 5549-5556.
- 18 Vuillaume, D.; Boulas, C.; Collet, J.; Davidovits, J. V.; Rondelez, F., *Appl. Phys. Lett.* **1996**, *69* (11), 1646-1648.
- 19 Dickey, M. D.; Chiechi, R. C.; Larsen, R. J.; Weiss, E. A.; Weitz, D. A.; Whitesides, G. M., *Advanced Functional Materials* **2008**, *18* (7), 1097-1104.
- 20 Selzer, Y.; Salomon, A.; Cahen, D., *J. Phys. Chem. B* **2002**, *106* (40), 10432-10439.
- 21 Vuillaume, D.; Boulas, C.; Collet, J.; Allan, G.; Delerue, C., *Physical Review B* **1998**, *58* (24), 16491-16498.)
- 22 Segev, L.; Salomon, A.; Natan, A.; Cahen, D.; Kronik, L., *Phys. Rev. B* **2006**, *74* (16), 6.

-
- 23 Mirjani, F.; Thijssen, J. M.; van der Molen, S. J., *Physical Review B* **2011**, *84* (11), 115402.
- 24 Nijhuis, C. A.; Reus, W. F.; Siegel, A. C.; Whitesides, G. M., *Journal of the American Chemical Society* **2011**, *133* (39), 15397-15411.
- 25 Pieterse, M. M. J.; Sluyters-Rehbach, M.; Sluyters, J. H., *Zeitschrift für Physikalische Chemie* **1978**, *113* (1), 117-124.
- 26 Richter, C. A.; Hacker, C. A.; Richter, L. J., *The Journal of Physical Chemistry B* **2005**, *109* (46), 21836-21841.
- 27 Linford, M. R.; Chidsey, C. E. D., *J. Am. Chem. Soc.* **1993**, *115* (26), 12631-12632.
- 28 Linford, M. R.; Fenter, P.; Eisenberger, P. M.; Chidsey, C. E. D., *Ibid.* **1995**, *117* (11), 3145-3155.
- 29 Seitz, O.; Böcking, T.; Salomon, A.; Gooding, J. J.; Cahen, D., *Langmuir : the ACS journal of surfaces and colloids* **2006**, *22* (16), 6915-22.
- 30 Maoz, R.; Sagiv, J., *J. Colloid and Interface Sciences* **1984**, *100* (2), 465-496.
- 31 Brzoska, J. B.; Shahidzadeh, N.; Rondelez, F., *Nature* **1992**, *360*, 719-721.
- 32 Chiechi, R. C.; Weiss, E. A.; Dickey, M. D.; Whitesides, G. M., *Angewandte Chemie International Edition* **2008**, *47* (1), 142-144.
- 33 Wang, G.; Kim, Y.; Na, S.-I.; Kahng, Y. H.; Ku, J.; Park, S.; Jang, Y. H.; Kim, D.-Y.; Lee, T., *The Journal of Physical Chemistry C* **2011**, *115* (36), 17979-17985.

-
- 34 Wang, G.; Kim, T.-W.; Jo, G.; Lee, T., *Journal of the American Chemical Society* **2009**, *131* (16), 5980-5985.
- 35 Noy, G.; Ophir, A.; Selzer, Y., *Angew. Chem. Int. Ed.* **2010**, *49* (33), 5734-5736.
- 36 Cui, X. D.; Zarate, X.; Tomfohr, J.; Sankey, O. F.; Primak, A.; Moore, A. L.; Moore, T. A.; Gust, D.; Harris, G.; Lindsay, S. M., *Nanotechnology* **2002**, *13*, 5-14.
- 37 Engelkes, V. B.; Frisbie, C. D., *The journal of physical chemistry B* **2006**, *110* (20), 10011-20.
- 38 Reus, W. F.; Thuo, M. M.; Shapiro, N. D.; Nijhuis, C. A.; Whitesides, G. M., *ACS Nano* **2012**.
- 39 Haag, R.; Rampi, M. A.; Holmlin, R. E.; Whitesides, G. M., *Journal of the American Chemical Society* **1999**, *121* (34), 7895-7906.
- 40 Boulas, C.; Davidovits, J. V.; Rondelez, F.; Vuillaume, D., *Phys. Rev. Lett.* **1996**, *76* (25), 4797-4800.)
- 41 Qi, Y.; Yaffe, O.; Tirosh, E.; Vilan, A.; Cahen, D.; Kahn, A., *Chemical Physics Letters* **2011**, *511* (4-6), 344-347.
- 42 Yaffe, O.; Qi, Y.; Scheres, L.; Puniredd, S. R.; Segev, L.; Ely, T.; Haick, H.; Zuilhof, H.; Vilan, A.; Kronik, L.; Kahn, A.; Cahen, D., *Physical Review B* **2012**, *85* (4), 045433.
- 43 Vazquez, H.; Oszwaldowski, R.; Pou, P.; Ortega, J.; Perez, R.; Flores, F.; Kahn, A., *Europhys. Lett.* **2004**, *65* (6), 802-808.

-
- 44 Vázquez, H.; Gao, W.; Flores, F.; Kahn, A., *Phys. Rev. B* **2005**, *71* (4), 4.
- 45 Kahn, A.; Koch, N.; Gao, W., *J. Polymer Sci.: Part B: Polymer Phys.* **2003**, *41*, 2529-2548.
- 46 Salomon, A.; Boecking, M.; Seitz, O.; Markus, T.; Amy, F.; Chan, C. K.; Zhao, W.; Cahen, D.; Kahn, A., *Adv. Mat.* **2007**, *19*, 445-450.
- 47 Salomon, A.; Boecking, M.; Chan, C. K.; Amy, F.; Girshevitz, O.; Cahen, D.; Kahn, A., *Phys. Rev. Lett.* **2005**, *95*, 266807.
- 48 Bâldea, I., *EPL (Europhysics Letters)* **2012**, *98* (1), 17010.
- 49 Dressendorfer, P. V.; Barker, R. C., *Applied Physics Letters* **1980**, *36* (11), 933-935.

Molecule/Electrode Interface Energetics in Molecular Junction: a “Transition Voltage Spectroscopy” Study

Guillaume Ricœur, Stéphane Lenfant^{}, David Guérin, Dominique Vuillaume^{*}*

Institut d'Electronique Microélectronique et Nanotechnologie (IEMN), CNRS, University of
Lille, B.P. 60069, Avenue Poincaré, F-59652, Villeneuve d'Ascq, France

^{*} To whom correspondence should be addressed. E-mail: dominique.vuillaume@iemn.univ-lille1.fr; stephane.lenfant@iemn.univ-lille1.fr

Supporting Information

Contact-Angle Measurements We measured the water contact angle with a remote-computer controlled goniometer system (DIGIDROP by GBX, France). We deposited a drop (10-30 μL) of deionized water ($18\text{M}\Omega\cdot\text{cm}^{-1}$) on the surface, and the projected image was acquired and stored by the computer. Contact angles were extracted by contrast contour image analysis software. These angles were determined a few seconds after application of the drop. These measurements were carried out in a clean room (ISO 6) where the relative humidity (50%) and the temperature (22 °C) are controlled. The precision with these measurements are $\pm 2^\circ$.

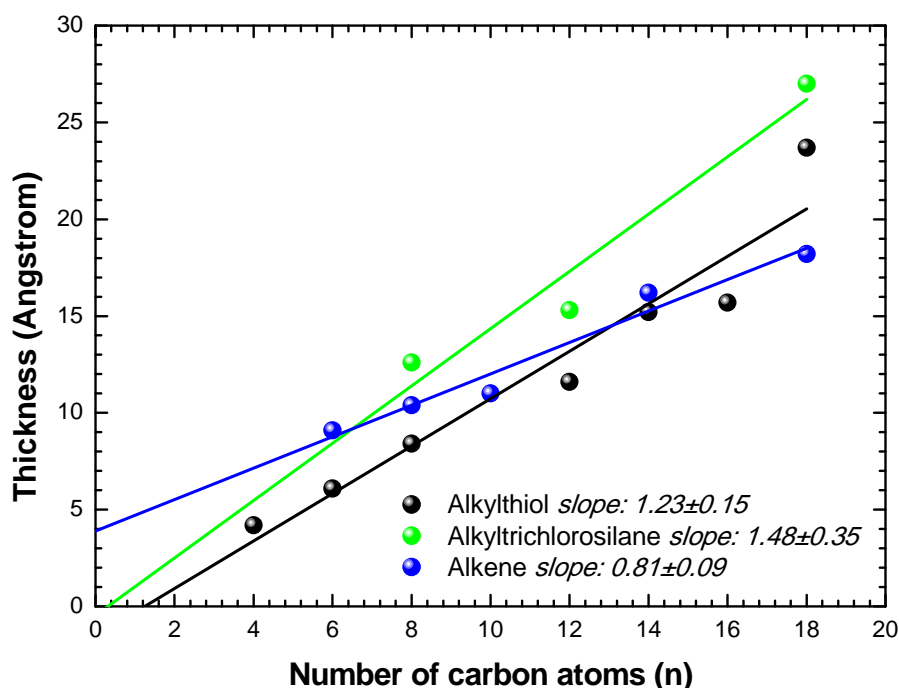
Spectroscopic Ellipsometry We recorded spectroscopic ellipsometry data in the visible range using an UVISSEL (Jobin Yvon Horiba) spectroscopic ellipsometer equipped with a DeltaPsi 2 data analysis software. The system acquired a spectrum ranging from 2 to 4.5 eV (corresponding to 300-750 nm) with intervals of 0.1 eV (or 15 nm). Data were taken at an angle of incidence of 70°, and the compensator was set at 45.0°. We fitted the data by a regression analysis to a film-on-substrate model as described by their thickness and their complex refractive indexes. First, we recorded a background before monolayer deposition. Second, after the monolayer deposition, we used a two-layer model (substrate/SAM) to fit the measured data and to determine the SAM thickness. We used the previously measured optical properties of the substrate (background), and we fixed the refractive index of the organic monolayer at 1.50. The usual values in the literature for the refractive index of organic monolayers are in the range 1.45 - 1.50 [1;2]. We can notice that a change from 1.50 to 1.55 would result in less than 1 Å error for a thickness less than 30 Å. We estimated the accuracy of the SAM thickness measurements at ± 1 Å.

Water contact angle and ellipsometric thicknesses measurements are presented below for the different SAMs:

Molecule / n carbon		4	6	8	10	12	14	16	18	Ref.
Alkyl-Thiol	e (Å)	4.2	6.1	8.4		11.6	15.2	15.7	23.7	
	Θ (°)	96°	102°	107°		109°	110°	79°	108°	99-108° [3]
Alkyl-Trichlorosilane	e (Å)			12.6		15.3			27	
	Θ (°)			108°		100°			112°	100-110° [4]
Alkene	e (Å)		9.1	10.4	11		16.2		18.2	
	Θ (°)		97	100	107		108		109	111° [5]

Table S1: Thicknesses measured by ellipsometry and water contact angles

For comparison, water contact angle measured on same self-assembled monolayers are presented with the associated reference. Thickness values are also presented in the graph below as a function of the number of carbon atom.



For alkyltrichlorosilane monolayers, the dependence with n the number of carbon atoms (the slope from the graph) is 1.48 ± 0.35 Å/methylene, a value closed to the one obtained by Wasserman *et al.* [4] (1.26 Å/methylene). For alkylthiol monolayers on gold surfaces, Porter *et al.* [6] measured a slope of 1.5 Å/methylene, close to the value measured here (1.23 ± 0.15 Å/methylene). In the case of alkene monolayer grafted on hydrogenated silicon, the slope measured here (0.81 ± 0.09 Å/methylene) is also close to the value obtained by Seitz and coworkers (1.0 Å/methylene) [5].

REFERENCES

- [1] Parikh, A. N.; Allara, D. L.; Ben Azouz, I.; Rondelez, F., An intrinsic relationship between molecular structure in self-assembled n-alkylsiloxane monolayers and deposition temperature. *J. Phys. Chem.* 1994, 98, 7577-7590.
- [2] Ulman, A., An introduction to ultrathin organic films: from Langmuir-Blodgett to Self-assembly. Academic press: Boston, 1991.
- [3] Delamarche, E. M., B; Kang, H.; Gerber, C., Thermal stability of self-assembled monolayers. *Langmuir* 1994, 10, 4103-4108.
- [4] Wasserman, S. R.; Tao, Y.; Whitesides, G. M., Structure and reactivity of alkylsiloxane monolayers formed by reaction of alkytrichlorosilanes on silicon substrates. *Ibid.* 1989, 5, 1074-1087.
- [5] Seitz, O.; Böcking, T.; Salomon, A.; Gooding, J. J.; Cahen, D., Importance of monolayer quality for interpreting current transport through organic molecules: alkyls on oxide-free Si. *Langmuir : the ACS journal of surfaces and colloids* 2006, 22 (16), 6915-22.
- [6] Porter, M. D.; Bright, T. B.; Allara, D. L.; Chidsey, C. E. D., Spontaneously organized molecular assemblies. 4. Structural characterization of n-alkyl thiol monolayers on gold by optical ellipsometry, infrared spectroscopy and electrochemistry. *J. Am. Chem. Soc.* 1987, 109 (12), 3559-3568.